

Mixing and CP violation in charm decays at LHCb

D. Červenkov on behalf of the LHCb collaboration
University of Oxford, United Kingdom.

Received 15 January 2022; accepted 23 February 2022

We present an overview of four recent measurements of charm decays performed at the LHCb experiment. These include the first observation of the non-zero mass difference between neutral charm-meson eigenstates, the most precise measurements of ΔY_{KK} and $\Delta Y_{\pi\pi}$, and time-integrated A_{CP} of eight two-body charm decays. The precision of the measurements is mainly limited by statistical uncertainty, so further improvement is expected with the upcoming LHC Run 3.

Keywords: High-energy physics; charm physics; mixing; CP violation; LHCb.

DOI: <https://doi.org/10.31349/SuplRevMexFis.3.0308061>

1. Introduction

Charm decays are the only up-type quark meson decays where CP violation (CPV) can be studied and are complementary to kaon and B -meson decays. However, our understanding of charm dynamics is severely limited by significant long-distance contributions and non-perturbative effects [1], which are notoriously difficult to predict and describe theoretically.

Recent years have seen a renaissance of charm physics fueled by a range of new results from various colliders (B-factories, the Tevatron, and the LHC). $D^0 - \bar{D}^0$ meson mixing is now a well-established phenomenon, and CP violation was observed in D^0 decays into two pions or two kaons in 2019 [2].

Mixing and CPV in charm are quite different from the same effects in the strange and beauty systems. Both effects are severely suppressed by the Glashow-Iliopoulos-Maiani mechanism and the magnitude of the Cabibbo-Kobayashi-Maskawa elements. Furthermore, the mass of the charm quark is close to the hadronic scale Λ_{QCD} , so the usual perturbative expansion in Λ_{QCD}/m_c is tricky. Finally, the magnitude of the strong running coupling α_s at the charm mass scale is large, which means higher-order contributions and non-perturbative effects can be significant. These points might sound rather negative, but the strong SM suppression also means the New Physics potential is great, and experimental input is crucial to constrain charm dynamics.

2. Formalism

Neutral meson mixing is a consequence of a mismatch between flavour and mass eigenstates. Labelling the mass eigenstates 1 and 2, we can write

$$|D_{1,2}\rangle = p|D^0\rangle \pm q|\bar{D}^0\rangle, \quad (1)$$

where p, q are complex numbers relating the flavour and mass eigenstates. The mixing parameters relate to the differences

between the two mass eigenstates. They are

$$x \equiv \Delta m_D/\Gamma_D \quad \text{and} \quad y \equiv \Delta\Gamma_D/2\Gamma_D, \quad (2)$$

where Δm_D and $\Delta\Gamma_D$ are the differences between the heavy and light eigenstates' mass and decay width, respectively. Γ_D is the average decay width. The factor of two in the second equation is a convention that creates a certain symmetry between the two parameters.

Three flavours of CPV exist, and all three are expected to be realised in charm:

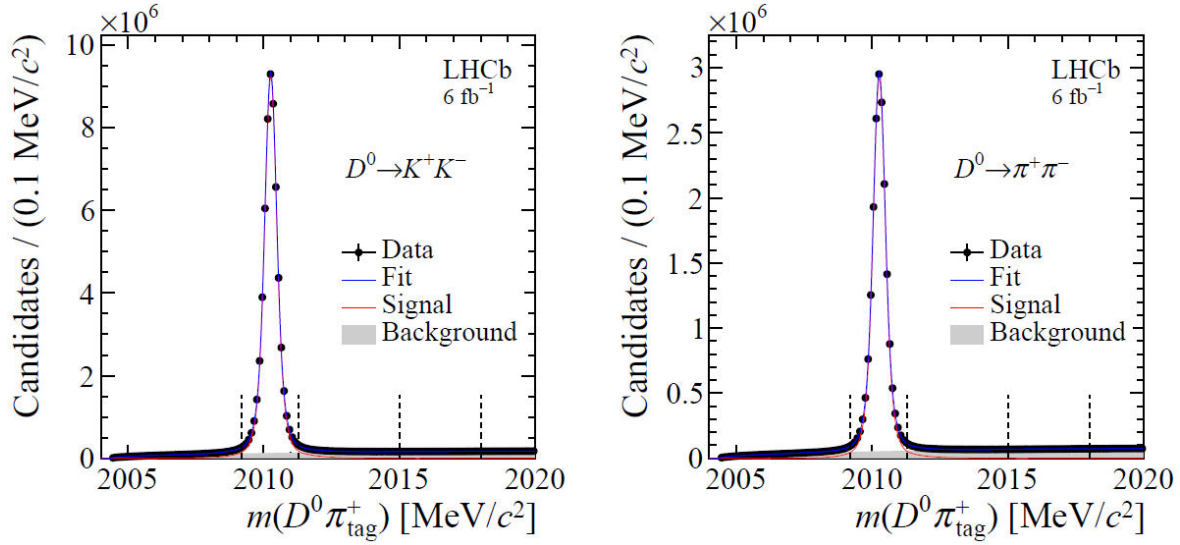
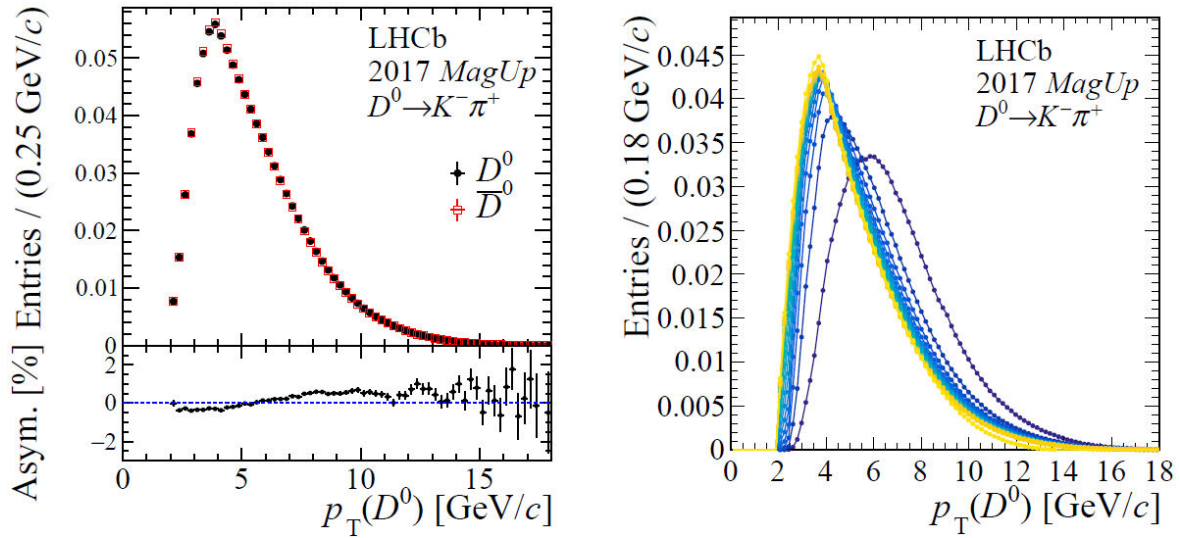
- CPV in decay occurs when the decay width for a $D^0 \rightarrow f$ decay is different than for the CP -conjugated $\bar{D}^0 \rightarrow \bar{f}$ decay.
- CPV in mixing appears when the probability of the $D^0 \rightarrow \bar{D}^0$ process is different from that of $\bar{D}^0 \rightarrow D^0$. It is characterized by $|q/p| \neq 1$.
- Finally, CPV can originate from the interference between decay and mixing. The relevant condition is $\phi_{\lambda_f} \equiv \arg(q\bar{A}_f/pA_f) \neq \{0, \pi\}$, where A_f and \bar{A}_f are the decay amplitudes of D^0 and \bar{D}^0 mesons, respectively, to a common final state f .

Traditionally, CPV in charm is characterized using $|q/p|$ and ϕ_{λ_f} . While the phase ϕ_{λ_f} depends on the final state, at current experimental precision, this effect is often neglected, thus taking $\phi \approx \phi_{\lambda_f}$.

An alternative CPV parametrisation is gaining popularity thanks to certain advantages it confers — the parameters offer better statistical properties and are easier for theorists to interpret. The alternative parameters are the CP -even mixing parameters x_{CP}, y_{CP} , which are approximately equal to the original x, y , and CPV parameters $\Delta x, \Delta y$ defined as

$$\Delta x = \frac{1}{2} \left[x \cos \phi \left(\left| \frac{q}{p} \right| - \left| \frac{p}{q} \right| \right) + y \sin \phi \left(\left| \frac{q}{p} \right| + \left| \frac{p}{q} \right| \right) \right], \quad (3)$$

$$\Delta y = \frac{1}{2} \left[y \cos \phi \left(\left| \frac{q}{p} \right| - \left| \frac{p}{q} \right| \right) - x \sin \phi \left(\left| \frac{q}{p} \right| + \left| \frac{p}{q} \right| \right) \right]. \quad (4)$$

FIGURE 1. Mass distributions of the D^* candidates.FIGURE 2. Transverse momentum distributions of the D^0 candidates in the $D^0 \rightarrow K^- \pi^+$ control channel. In the right plot, yellow (blue) represents low (high) decay times.

3. Search for time-dependent CPV in $D^0 \rightarrow h^+ h^-$ ($h \in \{K, \pi\}$)

A new measurement of time-dependent CPV in the $D^0 \rightarrow K^+ K^-$ and $D^0 \rightarrow \pi^+ \pi^-$ decays was recently performed at the LHCb [3]. These are the same channels that were used for the 2019 ΔA_{CP} discovery [2]. The D^0 was required to originate from a $D^* \rightarrow D^0 \pi_{\text{tag}}^+$ decay so that its flavour at production could be deduced from the charge of the tagging pion. The analysis used proton-proton collision data collected from 2015 to 2018 at a centre-of-mass energy of 13 TeV, corresponding to an integrated luminosity of 6 fb^{-1} . The data sample corresponds to 58 million and 18 million $D^0 \rightarrow K^+ K^-$ and $D^0 \rightarrow \pi^+ \pi^-$ candidates, respectively. The signal purity is around 95%, as can be seen in Fig. 1.

The observable is the time-dependent CP asymmetry which can be parametrised as

$$A_{CP}(t) \equiv \frac{\Gamma(D^0(t) \rightarrow f) - \Gamma(\bar{D}^0(t) \rightarrow f)}{\Gamma(D^0(t) \rightarrow f) + \Gamma(\bar{D}^0(t) \rightarrow f)} \quad (5)$$

$$= a_f^d + \Delta Y_f \frac{t}{\tau_D} + \mathcal{O}(x^2, y^2, xy),$$

where a_f^d is the CP asymmetry in the decay, τ_D is the D^0 lifetime, and ΔY_f is the parameter of interest that can be approximated as

$$\Delta Y_f \approx x \phi_{\lambda_f} - y \left(\left| \frac{q}{p} \right| - 1 \right) + y a_f^d, \quad (6)$$

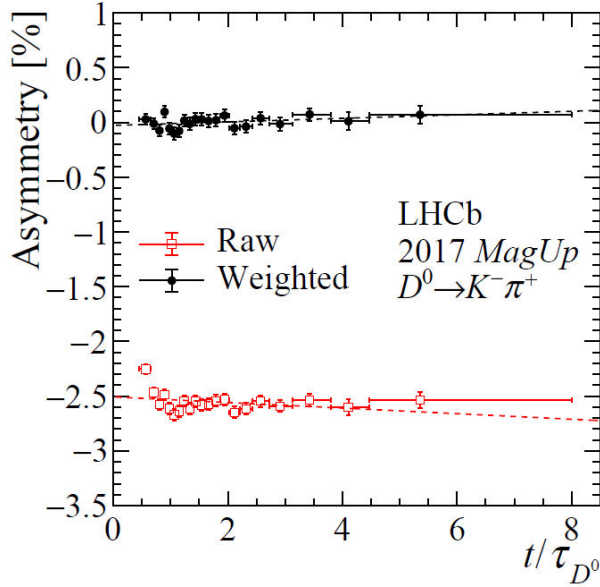


FIGURE 3. Time-dependent CP asymmetry of raw and weighted $D^0 \rightarrow K^- \pi^+$ control channel candidates.

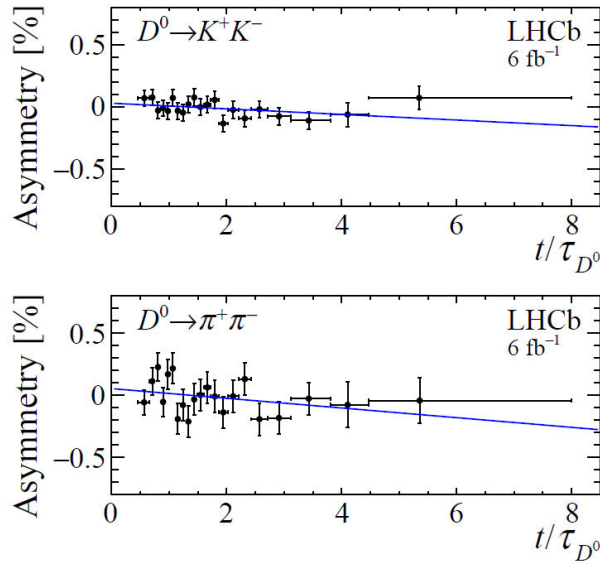


FIGURE 4. Time-dependent CP asymmetry fits of $D^0 \rightarrow K^+ K^-$ and $D^0 \rightarrow \pi^+ \pi^-$ candidates.

demonstrating that it receives contributions from all three types of CPV . Standard Model ΔY_f predictions are very small at 10^{-4} – 10^{-5} [4, 5].

The measured parameter is actually the asymmetry between D^0 and \bar{D}^0 yields.

$$A_{\text{raw}} = \frac{N(D^0(t) \rightarrow f) - N(\bar{D}^0(t) \rightarrow f)}{N(D^0(t) \rightarrow f) + N(\bar{D}^0(t) \rightarrow f)} \quad (7)$$

$$\approx a_f^d + \Delta Y_f \frac{t}{\tau_D} + A_{\text{prod}}(f, t) + A_{\text{det}}(f, t),$$

rather than A_{CP} . $A_{\text{prod}}(f, t)$ and $A_{\text{det}}(f, t)$ are time-dependent production and detection nuisance asymmetries.

The time-dependence of these parameters is brought on by the trigger requirements. Initially, there is a momentum-dependent detection asymmetry based on magnetic field polarity and charge of the tagging pion. There is also a production asymmetry because the LHC collides protons with protons, rather than antiprotons, so the quark-antiquark structure is not symmetric. The two described asymmetries result in a D^0/\bar{D}^0 momentum asymmetry. This asymmetry can be observed in the transverse momentum distributions of the $D^0 \rightarrow K^- \pi^+$ control channel shown in the left plot of Fig. 2. The trigger requirements then correlate D^0 decay time with kinematics and the nuisance asymmetries become time dependent. This is illustrated in the right plot of Fig. 2, where different colors represent different D^0 decay times.

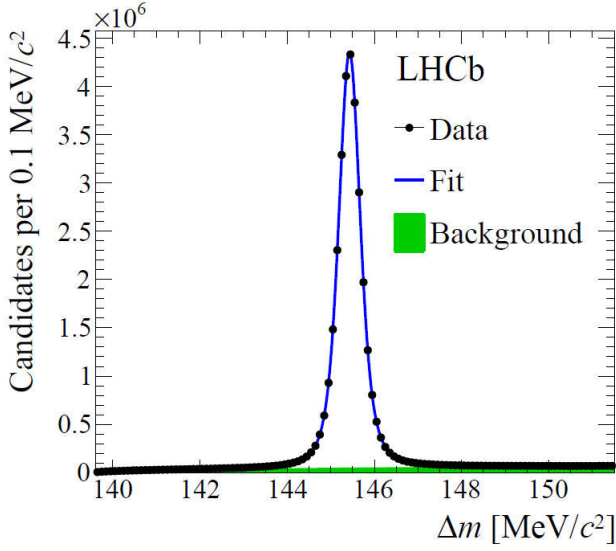
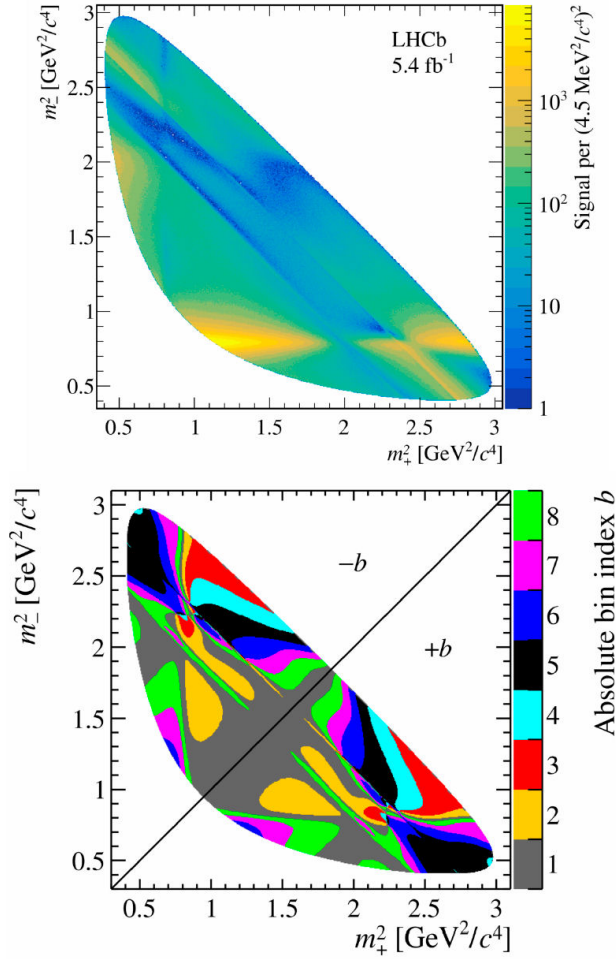
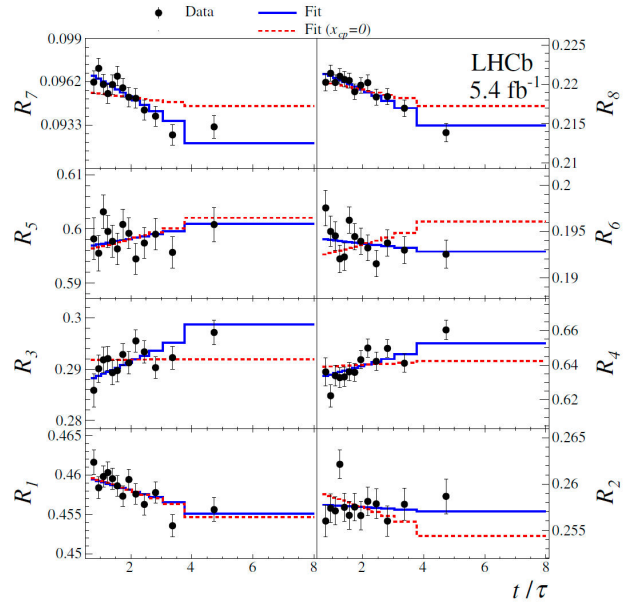
The solution to mitigate this problem is to equalise D^0/\bar{D}^0 kinematics by weighting the events. Figure 3 demonstrates the effect of this approach in the control channel, where no observable asymmetry is expected. The raw distribution exhibits apparent asymmetry and a non-zero slope. After the weighting procedure, no asymmetry in the control channel is observed, in line with expectations.

The final asymmetry fits are shown in Fig. 4. The results are $\Delta Y_{K^+ K^-} = (-2.3 \pm 1.5 \pm 0.3) \times 10^{-4}$ and $\Delta Y_{\pi^+ \pi^-} = (-4.0 \pm 2.8 \pm 0.4) \times 10^{-4}$, where the first uncertainty is statistical and second systematic. $\Delta Y_{K^+ K^-}$ and $\Delta Y_{\pi^+ \pi^-}$ agree with each other within 0.5σ . The agreement was expected as the final state dependence is predicted to be negligible. The results are also compatible with no CPV within 2σ . The precision of the results was improved by a factor of two compared with the previous measurement [6]. The results are dominated by statistical uncertainty, which means there are great prospects for future LHCb measurements. This is made even more exciting by the fact that the total uncertainty is approaching [7] the Standard Model prediction of 10^{-4} – 10^{-5} [4, 5].

4. Observation of the mass difference between neutral charm-meson eigenstates

The non-zero decay width difference between neutral charm mesons, y , has been established in the past years [8–10]. However, the mass difference, x , has so far been elusive. Its most precise past measurement was reported by LHCb as $x_{CP} = (2.7 \pm 1.6) \times 10^{-3}$ [11].

The measurement presented here [12] was optimised for x_{CP} precision, similarly to the previous measurement [11]. Much like the analysis of Sec. 3, it used D^0 from D^* decays. The events came from proton-proton collisions collected by the LHCb experiment from 2016 to 2018, corresponding to an integrated luminosity of 5.4 fb^{-1} . A total of 30.6 million $D^0 \rightarrow K_S^0 \pi^+ \pi^-$ decays were analysed. The mass difference Δm between the D^* and D^0 candidates is shown in Fig. 5. The Δm is a good variable because it subtracts D^0 resolution effects and leaves only the effects from the slow π .

FIGURE 5. Mass difference between the D^* and D^0 candidates.FIGURE 6. Dalitz plot (left) and binning (right) of $D^0 \rightarrow K_S^0 \pi^+ \pi^-$ candidates.FIGURE 7. CP -averaged yield ratios of $D^0 \rightarrow K_S^0 \pi^+ \pi^-$ candidates.

The analysis exploits the rich, resonant structure of the multi-body final state; see the left Dalitz plot in Fig. 6. Many interfering amplitudes such as $D^0 \xrightarrow{\text{DCS}} K^{*+} \pi^- \rightarrow K_S^0 \pi^+ \pi^-$ and $D^0 \xrightarrow{\text{mix}} \bar{D}^0 \xrightarrow{\text{CF}} K^{*+} \pi^- \rightarrow K_S^0 \pi^+ \pi^-$ contribute. The analysis employs the “bin-flip” method [13] which is optimised for x_{CP} sensitivity. The Dalitz plane is divided into positive and negative bins, mirrored across the diagonal. They are defined in such a way that the strong-phase D^0 - \bar{D}^0 difference varies minimally across each bin. The strong phases are constrained in the fit using CLEO and BES III inputs [14, 15]. The observables are the ratios of events in positive and negative bins. One of the method’s benefits is that most detector nuisance effects cancel in the ratio.

Time-dependent fits to the ratios of the eight bin pairs can be seen in Fig. 7. Deviations from a constant value are due to mixing. The red dashed lines are fit projections where x_{CP} was fixed to zero, which shows that y_{CP} alone cannot reproduce the observed distributions. The mixing parameters are measured to be $x_{CP} = (3.97 \pm 0.46 \pm 0.29) \times 10^{-3}$ and $y_{CP} = (4.59 \pm 1.20 \pm 0.85) \times 10^{-3}$, which is the first non-zero measurement of x_{CP} , with a significance larger than 7σ .

The analysis also looked at the difference of ratios for D^0 and \bar{D}^0 and observed no CPV . However, limits were improved considerably. The observed values were $\Delta x = (-0.27 \pm 0.18 \pm 0.01) \times 10^{-3}$ and $\Delta y = (0.20 \pm 0.36 \pm 0.13) \times 10^{-3}$. The world averages of both the charm mixing and CPV were improved significantly by this analysis as can be seen in Fig. 8, where the yellow (blue) contours show the current world average with (without) the presented measurement. Both Δx and Δy uncertainties are statistically dominated, leaving a clear path towards future improvement.

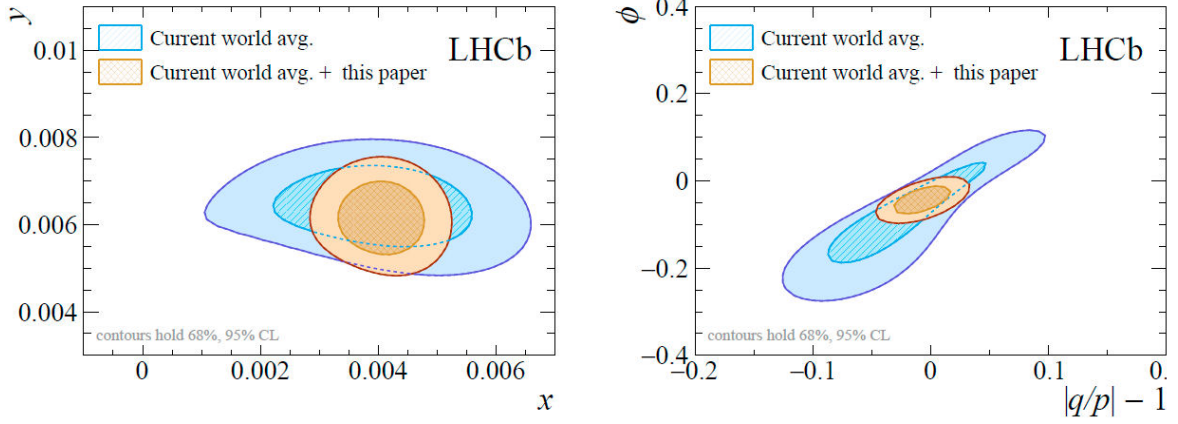


FIGURE 8. Global fits of charm mixing and CPV parameters with and without the presented $D^0 \rightarrow K_S^0 \pi^+ \pi^-$ analysis.

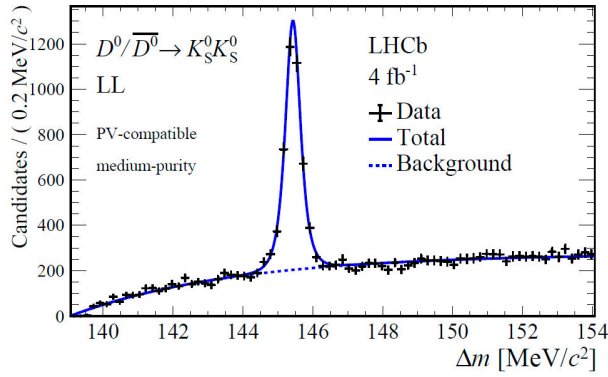


FIGURE 9. Mass difference between the D^* and D^0 candidates for the most significant sub-sample.

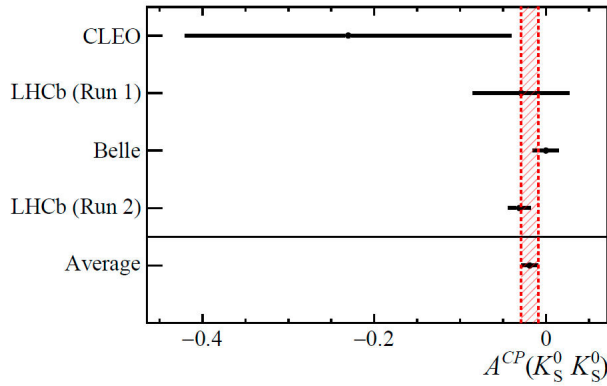


FIGURE 10. Previous and present measurements and world average of $A_{CP}(D^0 \rightarrow K_S^0 K_S^0)$.

5. Measurement of CP asymmetry in $D^0 \rightarrow K_S^0 K_S^0$ decays

The $D^0 \rightarrow K_S^0 K_S^0$ decay is ideal for CPV observation because the approximate U -spin symmetry can enhance the effect significantly; A_{CP} in this channel might be as large as 1% [16].

The presented analysis [17] boasts several enhancements over the previous analysis that used a smaller data set [18]. The nuisance production and detection asymmetries were removed by a weighting technique exploiting the $D^0 \rightarrow K^+ K^-$ calibration sample. The data was also split into consistent sub-samples based on mass resolution and purity. The new techniques resulted in a 30% sensitivity improvement at equal yields. Paired with the data set size increasing from 2 fb^{-1} to 6 fb^{-1} , this led to a significantly more precise measurement. The analysis extracted time-integrated A_{CP} from a 3D fit to $m(K_S^0)$ of both K_S^0 and $\Delta m = m(K_S^0 K_S^0 \pi^+) - m(K_S^0 K_S^0)$, which is shown in Fig. 9. The result is $A_{CP}(D^0 \rightarrow K_S^0 K_S^0) = (-3.1 \pm 1.2 \pm 0.4 \pm 0.2)\%$, where the first uncertainty is statistical, the second systematic and the last one comes from the control sample. The result is compatible with zero within 2.4σ and is the highest precision measurement of the parameter to date. Figure 10 shows the context and updated world average for $A_{CP}(D^0 \rightarrow K_S^0 K_S^0)$.

6. Search for CPV in $D_{(s)}^+ \rightarrow h^+ \pi^0$ and $D_{(s)}^+ \rightarrow h^+ \eta$, $h \in \{K, \pi\}$

The presented analysis [19] studied seven decays; those indicated in the Section title sans $D_s^+ \rightarrow \pi^+ \pi^0$, which is too highly suppressed. $A_{CP}(D^+ \rightarrow \pi^+ \pi^0)$ is negligible in the Standard Model because of isospin selection rules, making it a promising decay for New Physics searches. It is also noteworthy that this is the first measurement of $A_{CP}(D_{(s)}^+ \rightarrow h^+ h^0)$ at a hadron collider. Studying two-body decays with neutral particles in the final state at hadron colliders is challenging as a displaced D decay vertex, which is necessary for background suppression, cannot be formed using a single track. The analysis used converted $\gamma \rightarrow e^+ e^-$ and three-body $h^0 \rightarrow e^+ e^- \gamma$ decays. The former only rarely happens in the vertex detector, the latter suffers from a small branching fraction. However, put together there are enough events to extract the asymmetry from a 2D fit to $m(h^+ h^0)$ and $m(e^+ e^- \gamma)$, the projections of which are shown in Fig. 11.

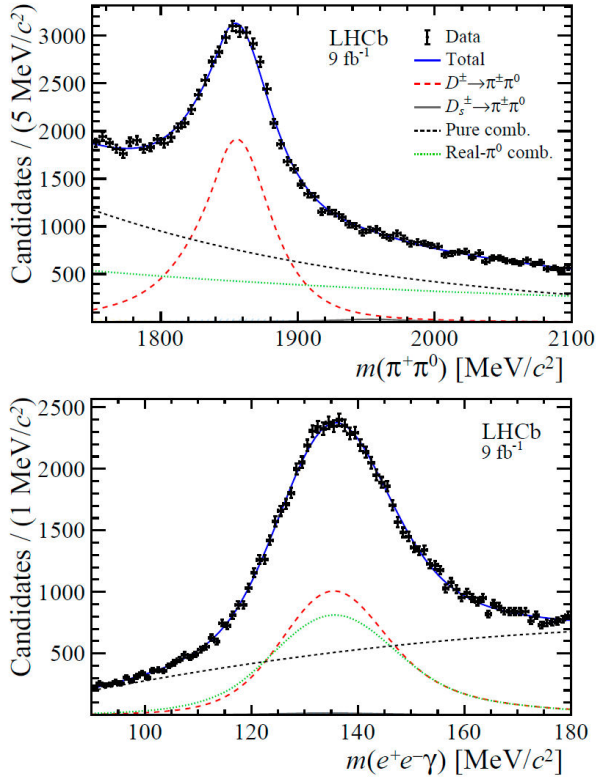


FIGURE 11. Mass distributions of D^0 (top) and h^0 (bottom) candidates.

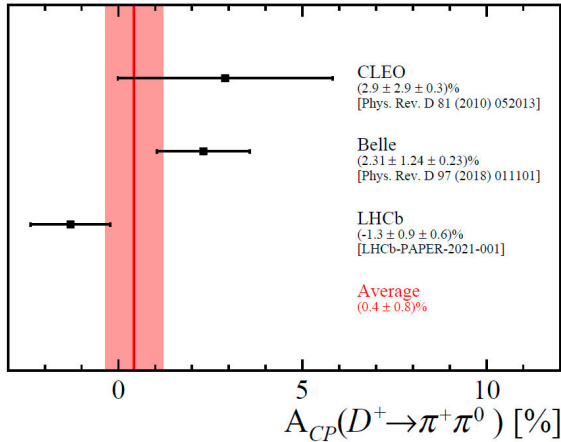


FIGURE 12. Past and present measurements and world average of $A_{CP}(D^+ \rightarrow \pi^+\pi^0)$.

TABLE I. A_{CP} results.

$A_{CP}(D^+ \rightarrow \pi^+\pi^0) = (-1.3 \pm 0.9 \pm 0.6)\%$
$A_{CP}(D^+ \rightarrow K^+\pi^0) = (-3.2 \pm 4.7 \pm 2.1)\%$
$A_{CP}(D^+ \rightarrow \pi^+\eta) = (-0.2 \pm 0.8 \pm 0.4)\%$
$A_{CP}(D^+ \rightarrow K^+\eta) = (-6 \pm 10 \pm 4)\%$
$A_{CP}(D_s^+ \rightarrow K^+\pi^0) = (-0.8 \pm 3.9 \pm 1.2)\%$
$A_{CP}(D_s^+ \rightarrow \pi^+\eta) = (0.8 \pm 0.7 \pm 0.5)\%$
$A_{CP}(D_s^+ \rightarrow K^+\eta) = (0.9 \pm 3.7 \pm 1.1)\%$

$D_{(s)}^+ \rightarrow K_S^0 h^+$ control samples were used to subtract production and detection asymmetries. A_{CP} of the control channels is known with a high precision [20] and was accounted for. The results are listed in Table I. All are compatible with CP symmetry, and the first five are the most precise measurements to date. Past and present measurements and the world average of $A_{CP}(D^+ \rightarrow \pi^+\pi^0)$ are shown in Fig. 12.

7. Conclusion

LHCb collected the largest sample of charm decays, which led to new world-best measurements of time-integrated CP asymmetries, including channels with neutrals in the final state, and time-dependent CP asymmetries and mixing parameters. The measurements include the first observation of a mass difference between neutral D mass eigenstates. The precision of the measurements is limited mainly by statistics, so further improvement is expected.

Many more intriguing LHCb results are sure to appear in the future, as there are more interesting Run 2 analyses in the pipeline and Run 3 will start this year, featuring a higher luminosity and an upgraded detector and trigger.

1. A. Lenz and G. Wilkinson. Mixing and CP Violation in the Charm System. *Annu. Rev. Nucl. Part. Sci.*, **71** (2021) 59, <https://doi.org/10.1146/annurev-nucl-102419-124613>.
2. (LHCb Collaboration) R. Aaij *et al.*, Observation of CP Violation in Charm Decays. *Phys. Rev. Lett.* **122** (2019) <https://doi.org/10.1103/physrevlett.122.211803>.
3. (LHCb Collaboration) R. Aaij *et al.* Search for time-dependent CP violation in $D^0 \rightarrow K^+K^-$ and $D^0 \rightarrow \pi^+\pi^-$ decays *Physical Review D* **104** (2021) <https://doi.org/10.1103/physrevd.104.072010>.
4. A. L. Kagan and L. Silvestrini, Dispersive and absorptive CP violation in $D^0 - \bar{D}^0$ mixing, *Phys. Rev. D* **103** (2021) 053008, <https://doi.org/10.1103/>

- PhysRevD.103.053008.
5. H. Li, H. Umeeda, F. Xu, and F. Yu, D meson mixing as an inverse problem. *Physics Letters B*, **810** (2020) 135802, <https://doi.org/10.1016/j.physletb.2020.135802>.
 6. (LHCb Collaboration) R. Aaij *et al.*, Measurement of the CP Violation Parameter A_Γ in $D^0 \rightarrow K^+K^-$ and $D^0 \rightarrow \pi^+\pi^-$ Decays, *Physical Review Letters*, **118** (2017), <https://doi.org/10.1103/physrevlett.118.261803>.
 7. (LHCb Collaboration) R. Aaij *et al.* Expression of Interest for a Phase-II LHCb Upgrade: Opportunities in flavour physics, and beyond, in the HL-LHC era. Technical report, CERN, Geneva, Feb 2017. <https://cds.cern.ch/record/2244311>.
 8. (BABAR Collaboration) J. P. Lees *et al.*, Measurement of $D^0-\bar{D}^0$ mixing and CP violation in two-body D^0 decays *Phys. Rev. D* **87** (2013) 012004, <https://doi.org/10.1103/PhysRevD.87.012004>.
 9. (Belle Collaboration) M. Starič *et al.*, Measurement of $D^0 - \bar{D}^0$ mixing and search for CP violation in $D^0 \rightarrow K^+K^-, \pi^+\pi^-$ decays with the full Belle data set. *Physics Letters B*, **753** (2016) 412, <https://doi.org/10.1016/j.physletb.2015.12.025>.
 10. (LHCb Collaboration) R. Aaij *et al.*, Measurement of the Charm-Mixing Parameter y_{CP} , *Phys. Rev. Lett.*, **122** (2019) 011802, <https://doi.org/10.1103/PhysRevLett.122.011802>.
 11. (LHCb Collaboration) R. Aaij *et al.*, Measurement of the mass difference between neutral charm-meson eigenstates. *Phys. Rev. Lett.* **122** (2019) 231802, <https://doi.org/10.1103/PhysRevLett.122.231802>.
 12. (LHCb Collaboration) R. Aaij *et al.*, Observation of the Mass Difference between Neutral Charm-Meson Eigenstates. *Phys. Rev. Lett.* **127** (2021), <https://doi.org/10.1103/physrevlett.127.111801>.
 13. A. Di Canto *et al.*, Novel method for measuring charm-mixing parameters using multibody decays. *Phys. Rev. D* **99** (2019) 012007, <https://doi.org/10.1103/PhysRevD.99.012007>.
 14. (CLEO Collaboration) J. Libby *et al.*, Model-independent determination of the strong-phase difference between D^0 and $\bar{D}^0 \rightarrow K_{S,L}^0 h^+ h^-$ ($h = \pi, K$) and its impact on the measurement of the CKM angle γ/ϕ_3 , *Phys. Rev. D*, **82** (2010) 112006, <https://doi.org/10.1103/PhysRevD.82.112006>.
 15. (BESIII Collaboration) M. Ablikim *et al.*, Model-independent determination of the relative strong-phase difference between D^0 and $\bar{D}^0 \rightarrow K_{S,L}^0 \pi^+ \pi^-$ and its impact on the measurement of the CKM angle γ/ϕ_3 *Phys. Rev. D*, **101** (2020) 112002, <https://doi.org/10.1103/PhysRevD.101.112002>.
 16. U. Nierste and S. Schacht, CP violation in $D^0 \rightarrow K_S K_S$ *Phys. Rev. D* **92** (2015) 054036, <https://doi.org/10.1103/PhysRevD.92.054036>.
 17. (LHCb Collaboration) R. Aaij *et al.*, Measurement of CP asymmetry in $D^0 \rightarrow K_S^0 K_S^0$ decays, *Physical Review D*, **104** (2021) <https://doi.org/10.1103/physrevd.104.1031102>.
 18. (LHCb Collaboration) R. Aaij *et al.*, Measurement of the time-integrated CP asymmetry in $D^0 \rightarrow K_S^0 K_S^0$ decays, *Journal of High Energy Physics* **2018** (2018) [https://doi.org/10.1007/jhep11\(2018\)048](https://doi.org/10.1007/jhep11(2018)048).
 19. (LHCb Collaboration) R. Aaij *et al.*, Search for CP violation in $D_{(s)}^+ \rightarrow h^+ \pi^0$ and $D_{(s)}^+ \rightarrow h^+ \eta$ decays *Journal of High Energy Physics* **2021** (2021) [https://doi.org/10.1007/jhep06\(2021\)019](https://doi.org/10.1007/jhep06(2021)019).
 20. (LHCb Collaboration) R. Aaij *et al.*, Search for CP Violation in $D_s^+ \rightarrow K_S^0 \pi^+$, $D^+ \rightarrow K_S^0 K^+$, and $D^+ \rightarrow \phi \pi^+$ Decays *Phys. Rev. Lett.* **122** (2019) 191803